energies

MDPI

Article

Novel Auto-Reclosing Blocking Method for Combined Overhead-Cable Lines in Power Networks

Ricardo Granizo Arrabé [1,*], Carlos Antonio Platero Gaona [1], Fernando Álvarez Gómez [2] and Emilio Rebollo López [1]

[1] Department of Electrical Engineering, ETS Ingenieros Industriales, Technical University of Madrid, C/José Gutierrez Abascal, 2, 28006 Madrid, Spain; carlosantonio.platero@upm.es (C.A.P.G.); emilio.rebollo.lopez@gmail.com (E.R.L.)

[2] Department of Electrical Engineering, ETS Ingeniería y Diseño Industrial, Technical University of Madrid, C/Ronda de Valencia, 3, 28012 Madrid, Spain; fernando.alvarez@upm.es

* Correspondence: ricardo.granizo@upm.es; Tel.: +34-91-336-6842

Academic Editor: Miguel Castilla
Received: 25 June 2016; Accepted: 15 November 2016; Published: 17 November 2016

Abstract: This paper presents a novel auto-reclosing blocking method for combined overhead-cable lines in power distribution networks that are solidly or impedance grounded, with distribution transformers in a delta connection in their high-voltage sides. The main contribution of this new technique is that it can detect whether a ground fault has been produced at the overhead line side or at the cable line side, thus improving the performance of the auto-reclosing functionality. This localization technique is based on the measurements and analysis of the argument differences between the load currents in the active conductors of the cable and the currents in the shields at the cable end where the transformers in delta connection are installed, including a wavelet analysis. This technique has been verified through computer simulations and experimental laboratory tests.

Keywords: ground faults; protection; distribution protections; electrical distribution networks

1. Introduction

Power systems use protection devices to detect and clear different types of short circuits, overloads and, in general, abnormal working conditions or fault situations that might be dangerous to the facilities and the stability of the electrical power system. Most faults in power distribution networks are located in the lines those that take place in the machinery, switchgear and measurement devices installed at the main substations. Some distribution lines have two different parts: the cable line side and the overhead line side [1]. Protection relays have the responsibility to clear faults that happen in their protection zones and for that purpose, a close and quite approximate location of the ground fault in electrical power systems is required for protection systems [2]. Overhead protection systems have different working principles to cable protection systems [3]. At any distribution line, the protection system must guarantee the power supply in the most reliable way. For that purpose, there are many protection functions implemented to clear up all types of possible faults and keep the grid as stable as possible. Power distribution networks normally have voltage levels up to 45 kV although in some countries in Europe their voltage levels can reach up to 150 kV [4]. If there is a ground fault, a three-phase tripping order will be given to clear it, and a loss of power demand results [5]. It is extremely important to know the maximum reclosing time [6,7] to recover power supply and keep the system as stable as possible.

When a distribution line is formed by cable and overhead sections (Figure 1), faults in the cable line side cause irreparable damage because the insulation of the cable has been partially or totally deteriorated: this is the reason why reclosing attempts are not allowed. Faults at the overhead line side are normally produced by lightning strikes [8]. On the other hand, faults in the overhead line side

permit reclosing without risk, because the air insulation is normally recovered in a few milliseconds and almost one second if there is mutual capacitive coupling to other lines.

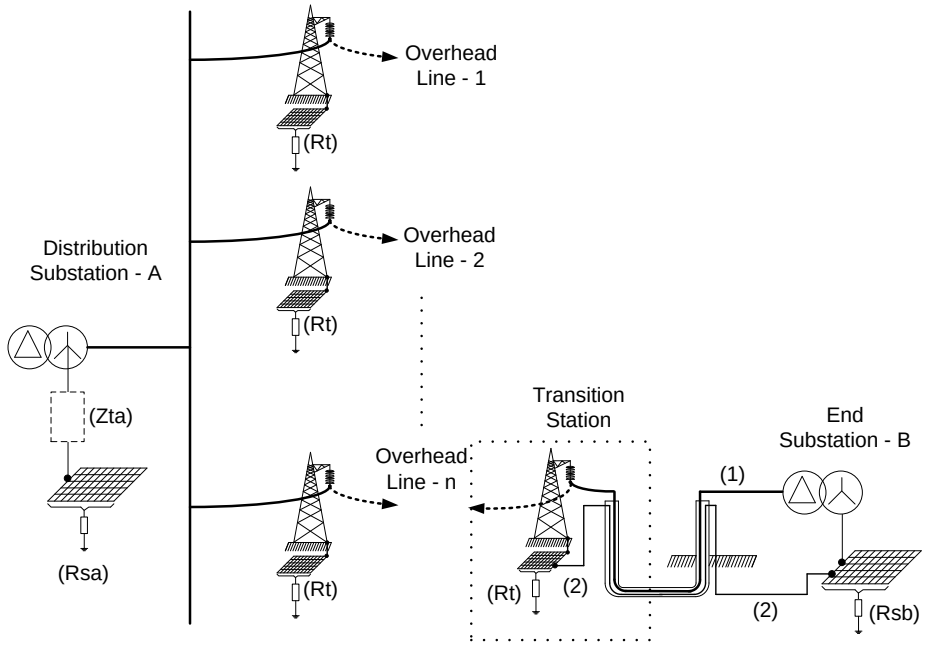

Figure 1. Power distribution network with transition cable-overhead line. (1) Active conductor of power cables; (2) Shields of the power cable; (R_t) Tower ground resistance; (R_{sa}) Ground resistance of distribution substation-A; (R_{sb}) Ground resistance of end substation-B; (Z_{ta}) Grounding impedance.

In Figure 1, the earthing of the cable shields at the transition station is connected to of the corresponding tower, whose earthing resistance value is represented as R_t. Substations A and B have their respective grounding resistances R_{sa} and R_{sb}. The earthing resistances R_t at every tower have normally slightly different values.

If a fault occurs at the cable line side and is cleared up, a post-reclosing order on the fault condition will be an unsuccessful reclosing maneuver. Also, the grid will have to withstand a new fault condition and be able to clear it up again. Beside these two disadvantages of unsuccessful reclosing maneuvers, another is the fact of creating significant and extensive damage in the cable, being the most probable consequence to have to replace it entirely. This circumstance will keep the distribution line out of order for a long time while the cable is replaced. Therefore, the discrimination of the fault in the overhead side or in the line side is essential to allow to protection and the control system to send a reclosing order [9]. Currently, there are different protection criteria to remove from service a line with a ground fault.

This presents a technique that determines where the ground fault has taken place in an overhead-cable line considering a grounding method mostly used in power distribution networks with the overhead side substations solidly grounded, or through grounding impedance with low ohmic value. At the cable end side, the system is ungrounded with power transformers in a delta connection in their primary side. The models used follow the impedance calculation described in the standard EN60909-3 [10].

We first present a brief overview of line protection techniques. Section 2 describes the formulation used for modeling the cables. Section 3 includes the impedances of cables and general equations for shield connections. Then, Section 4 details the principles of the proposed auto-reclosing blocking method technique. Section 5 analyzes the software simulations of the operation of the proposed method, and Section 6 presents the results of experimental fault tests carried out in the laboratory. Finally, Section 7 concludes with the main contributions of the proposed technique.

2. State-of-the-Art

There are two main protection relays that incorporate the auto-reclosing facility in power distribution networks: distance and ground fault directional overcurrent protection relays. In this section, both techniques are presented.

2.1. Distance Protection (ANSI 21)

This protection responds to the impedance value measured between the relay and the fault location [11–13]. As the impedance of any line is fairly constant, such protection relays work with the impedance value of the line. Its application requires consideration of several very important factors:

- The resistance of the arc [14].
- The different contributions to the short circuit current from the ends of the line.
- The effect of non-transposition of the conductors.
- The effect of zero sequence mutual impedance in parallel lines.

Among the most interesting features from the point of view of their application are:

- The reduction of the clearing times of faults.
- An easier coordination with other protections.
- The lack of sensitivity to power swings or pendulums in the network.

The locus of the action limit of the protection is the impedance seen by it. As this impedance is a complex number with a real part (resistance) and an imaginary part (reactance), it can be perfectly represented in *R*-*X* diagrams. Therefore, the tripping characteristic of the distance relay can be superimposed on an *R*-*X* diagram to the impedance seen by the same at fault condition, power swings or heavy loads, and thus be able to verify the performance of the protection. Figure 2 shows a typical setting of distance protection in a distribution line with line impedance Z_L with three impedance steps: Z_A, Z_B and Z_C. The tripping times for such zones are t_A, t_B, t_C with $t_A < t_B < t_C$.

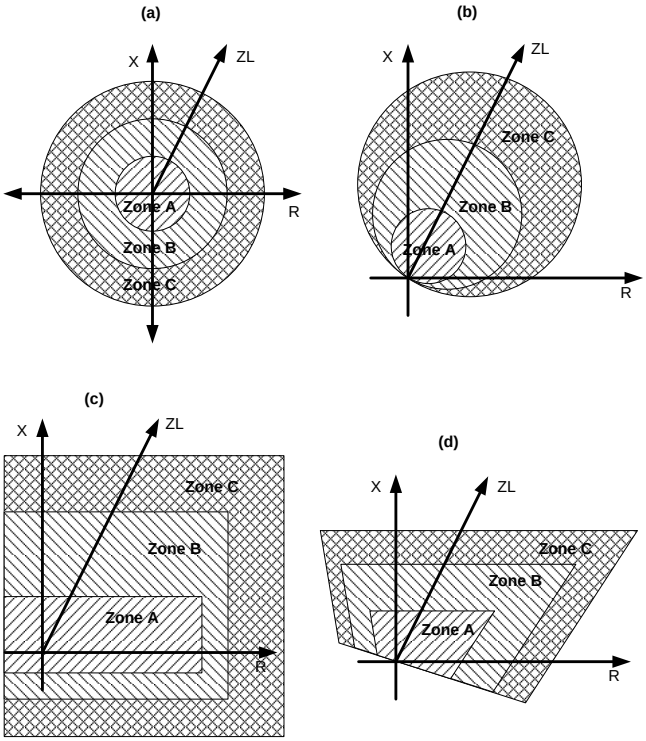

Figure 2. Types of impedance relay characteristics with three zone settings: (**a**) Impedance relay; (**b**) Mho relay; (**c**) Reactance relay; (**d**) Quadrilateral relay.

Any small current or voltage transformer error could represent an important increase or decrease in the measured impedance. Consequently, if the fault was produced very close to the transition overhead-cable line, it is not known in which side it has happened. Therefore, impedance protection is not fully selective to discriminate whether the ground fault has happened in the cable or in the overhead side. In power distribution networks rated 45 or 66 kV, distance protection is mainly used when the system is solidly grounded.

2.2. Directional Ground Fault Protection (ANSI 67N)

This protection measures the magnitudes of the ground fault current, the residual voltage and the angular difference between them. If the ground fault current and the residual voltage have values over the setting values previously set in the protection relay, and the angular difference between them is inside the directional tripping zone defined, the protection relay will send a tripping order to the circuit breaker once the tripping time set has expired. Most ground faults in solidly grounded power distribution networks have an inductive character; therefore, the characteristic angle between the ground fault current and residual voltage, at which the greatest sensitivity is achieved, is normally 110° with the ground fault current leading the residual voltage. Figure 3 shows the characteristic tripping zone for solidly grounded distribution power systems.

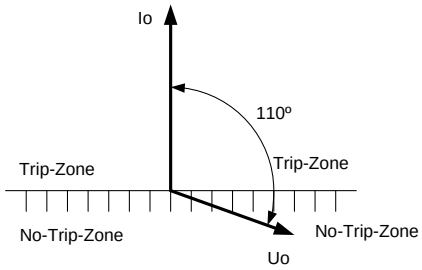

Figure 3. Tripping zone for solidly grounded power distribution networks. (Uo) Residual voltage; (Io) Residual current; (110°) Characteristic tripping angle.

3. Impedances of Cables and General Equations for Shield Connections

The proposed method applies to distribution lines with overhead and cable sections, where the shields of the cables are connected to earth at both ends of the cable, known as Single Bonding (SB). No transposition of the cable shields has been implemented [15]. For example, the composition of any standard cable for medium-voltage applications and a flat disposal of three cables are represented in Figure 4.

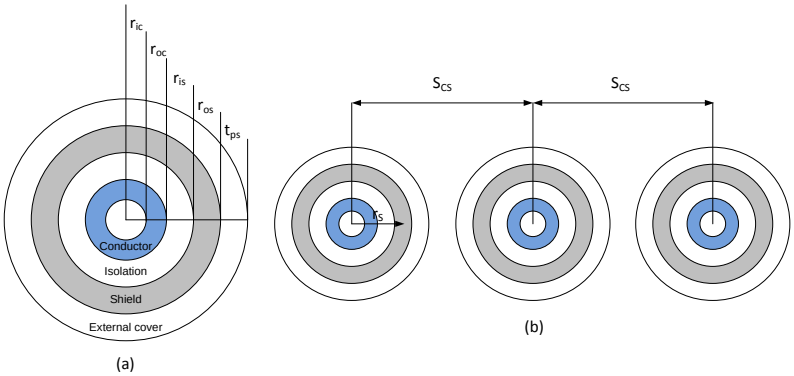

Figure 4. (**a**) Cable composition and (**b**) flat disposal. (r_{ic}) Internal conductor radius; (r_{oc}) External conductor radius; (r_{is}) Internal conductor shield; (r_{os}) External shield radius; (r_s) Average shield radius; (S_{CS}) Distance between axes of the conductor and shield; (t_{ps}) External cover thickness.

3.1. Impedance of Cable and Shields

In this section, the formulation that evaluates the impedances and self-impedances between the different parts of the cables is listed and implemented in Matlab to develop the cable models in Simulink used in the simulations described in Section 5. First, the self impedances of the conductors and shields are indicated. Then, the mutual impedances between them are calculated. Their impedance values are calculated using Carson's equations considering the effect of the return ground path for all types of self and mutual impedances.

The self impedance of the conductor is:

$$Z_C = R_{C(ca)} + \pi^2 \cdot 10^{-7} \cdot f + j \cdot 4 \cdot \pi \cdot 10^{-7} \cdot \ln(D_e / r_{oc}) \quad (1)$$

The expression for the return ground path distance given by Carson is:

$$D_e = 1.85 \cdot \sqrt{\frac{\rho_e}{\omega \cdot \mu_o}} \quad (2)$$

On the other hand, the self impedance of the shield is:

$$Z_S = R_{S(ca)} + \pi^2 \cdot 10^{-7} \cdot f + j \cdot 4 \cdot \pi \cdot 10^{-7} \cdot \ln(D_e / r_s) \quad (3)$$

The mutual impedance between conductor "i" and shield "j" can be written as:

$$Z_{CS} = \pi^2 \cdot 10^{-7} \cdot f + j \cdot 4 \cdot \pi \cdot 10^{-7} \cdot \ln(D_e / S_{CS}) \quad (4)$$

The mutual impedance between any conductor and its shield can be written as:

$$Z_{CS} = \pi^2 \cdot 10^{-7} \cdot f + j \cdot 4 \cdot \pi \cdot 10^{-7} \cdot \ln(D_e / r_s) \quad (5)$$

The mutual impedance between shields is given by:

$$Z_{SS} = \pi^2 \cdot 10^{-7} \cdot f + j \cdot 4 \cdot \pi \cdot 10^{-7} \cdot \ln(D_e / S_{SS}) \quad (6)$$

3.2. Balanced System: General Equations for Single Bonding (SB) Shield Connections

The circuit used in this study is shown in Figure 5 and corresponds to an SB connection.

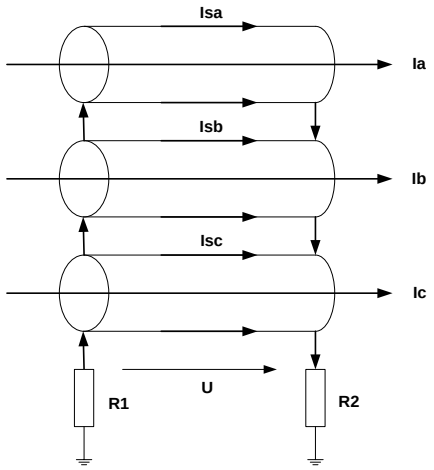

Figure 5. Standard shields connection for SB applications. (I_a, I_b, I_c) Currents in conductors; (I_{sa}, I_{sb}, I_{sc}) Currents in shields; (R_1, R_2) Ground resistances at both ends of shields; (U) Potential difference between shield terminals.

When the load currents form a three-phase balanced system and only a positive sequence component exists, the vector sum of the line currents flowing in the conductors is zero. The voltages induced in the shields have a component due to the flow of current through conductor, and another due to the currents circulating in the shields. As shown in Figure 5, the shields are grounded at both ends and the voltages between the two grounding connections are equal to the three shields as:

$$U = U_{1C} + U_{1S} = U_{2C} + U_{2S} = U_{3C} + U_{3S} \quad (7)$$

The mathematical models for such induced voltages are listed below:

- Induced voltages in shields due to circulating currents in conductors:

$$U_{1C} = L\cdot(Z_{C1S1}\cdot I_1 + Z_{C2S1}\cdot I_2 + Z_{C3S1}\cdot I_3) \quad (8)$$

$$U_{2C} = L\cdot(Z_{C1S2}\cdot I_1 + Z_{C2S2}\cdot I_2 + Z_{C3S2}\cdot I_3) \quad (9)$$

$$U_{3C} = L\cdot(Z_{C1S3}\cdot I_1 + Z_{C2S3}\cdot I_2 + Z_{C3S3}\cdot I_3) \quad (10)$$

- Induced voltages in shields due to circulating currents in shields:

$$U_{1S} = L\cdot(Z_{S1S1}\cdot I_{S1} + Z_{S2S1}\cdot I_{S2} + Z_{S3S1}\cdot I_{S3}) \quad (11)$$

$$U_{2S} = L\cdot(Z_{S1S2}\cdot I_{S1} + Z_{S2S2}\cdot I_{S2} + Z_{S3S2}\cdot I_{S3}) \quad (12)$$

$$U_{3S} = L\cdot(Z_{S1S3}\cdot I_{S1} + Z_{S2S3}\cdot I_{S2} + Z_{S3S3}\cdot I_{S3}) \quad (13)$$

All the previous equations can be expressed as a matrix system:

$$\begin{pmatrix} U_1 \\ U_2 \\ U_3 \end{pmatrix} = \begin{pmatrix} U_{1C} \\ U_{2C} \\ U_{3C} \end{pmatrix} + \begin{pmatrix} U_{1S} \\ U_{2S} \\ U_{3S} \end{pmatrix} \quad (14)$$

where:

$$\begin{pmatrix} U_1 \\ U_2 \\ U_3 \end{pmatrix} = L\cdot\begin{pmatrix} Z_{C1S1} & Z_{C2S1} & Z_{C3S1} \\ Z_{C1S2} & Z_{C2S2} & Z_{C3S2} \\ Z_{C1S3} & Z_{C2S3} & Z_{C3S3} \end{pmatrix}\cdot\begin{pmatrix} I_1 \\ I_2 \\ I_3 \end{pmatrix} + L\cdot\begin{pmatrix} Z_{S1S1} & Z_{S2S1} & Z_{S3S1} \\ Z_{S1S2} & Z_{S2S2} & Z_{S3S2} \\ Z_{S1S3} & Z_{S2S3} & Z_{S3S3} \end{pmatrix}\cdot\begin{pmatrix} I_{S1} \\ I_{S2} \\ I_{S3} \end{pmatrix} \quad (15)$$

4. Principles of Novel Auto-Reclosing Blocking Method for Power Distribution Networks

The new method presented measures the currents at the three shields of the cables at their ends located at the substation side, and the currents in the active part of the three phases of the cable as indicated in Figure 6. This was studied for solidly or low-value impedance grounded power distribution networks with distribution transformers in a delta connection at their high-voltage sides. This method is valid when the transition overhead-cable is not very far away from the substation where the measurements of currents in shields and conductors are done. We employ a trigger signal to start the analysis and consider a total time signal length of 40 ms as a pre-trigger time and 40 ms active fault time. The trigger signal is provided by any protection relay when a ground fault has been detected. The time set 40 ms for the active fault time is acceptable, as the ground faults at power distribution networks are active for longer times and the minimum tripping time for standard overcurrent or voltage relays is 30 ms. Apart from this time, the medium-voltage circuit breaker opening times are not less than 40–50 ms. This means that 40 ms as an active fault time is good enough, as will be verified in the simulation and real test results.

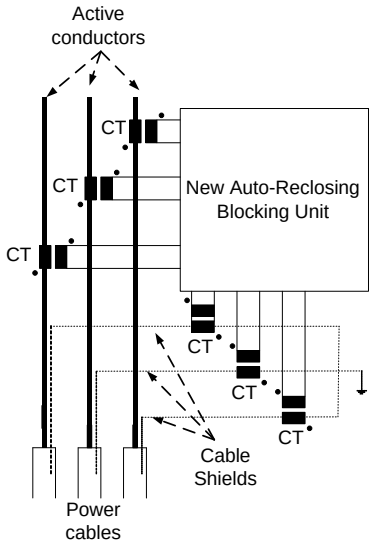

Figure 6. Currents of the cables measured in the active conductors and their shields.

Once this trigger signal has been acknowledged, the new method initiates the procedure to classify where the ground fault has happened, and takes the decision of whether or not to block the reclosing maneuver. With the shields connected in SB disposal, the new method first evaluates the angular difference between the currents in the active part of the cables and their corresponding shields during a time of 40 ms previous to the acknowledgement of the trigger, and another 40 ms after such trigger has been acknowledged, so the total evaluation time is 80 ms. A full period Fourier transformation over a running window of two cycles of the fundamental frequency to calculate the phase of the respective current. This angular difference is hereafter denoted as ΔL1S1, ΔL2S2 and ΔL3S3 for the respective phases and corresponding shields. A second evaluation is developed for the second decision criteria and to make sure that the right maneuver will be taken up. This second evaluation is a wavelet analysis of those angular differences. The wavelet analysis uses the discrete wavelet transform (DWT) and only evaluates the high-frequency elements [16–18]. These two analyses are now described.

4.1. Analysis of Angular Difference Between the Conductor Currents and Respective Shields

This analysis evaluates the angular differences ΔL1S1, ΔL2S2 and ΔL3S3. In normal operation without ground faults, the currents circulating in staggered cables in the three shields form a balanced system, and the angular differences between active currents and shield currents have similar values. Cables in flat disposal have unbalanced currents in the shields, as the distances between them are not exactly the same; whereas cables in delta disposal normally have very similar currents. As a function of the ground fault position, the phase-shield current angular differences are increased, decreased or stay the same. Their behavior allows, in most cases, the location of the ground fault to be determined. Typical overhead lines up to 30 km and cable lengths up to 1200 m have been evaluated as a case study. However, this method could be used in similar configurations with larger distances.

When the ground fault occurs in the overhead line side, the currents in the shields are due to the mutual coupling between all conductors and shields. In such ground fault conditions, the angular difference between them is in the range from 10 to 50°. Practically all ground fault current circulates from the fault point to the grounding system in the main distribution substation to which the power transformer is grounded.

However, if the ground fault occurs in the line side, ground fault current circulates from the fault point to both ends of the shield of the phase with a fault. The shield of the cable with the ground fault acts as a ground fault current divider. At the earthing of such a shield at both cable ends, both fault currents return to the main substation; whereas the currents circulating in the shields of the phases

without any fault keep circulating from one end to the other of the cable. This circulation process makes ΔL1S1, ΔL2S2 and ΔL3S3 greatly increase and have values well above 50° The threshold to decide whether the auto-reclosing maneuver is blocked has been selected as 50°, which appears in the algorithm developed for this new application.

4.2. Wavelet Analysis of the Angular Difference Between the Conductor Currents and Respective Shields

The use of wavelet analysis allows information in the time domain. The signal to be studied is decomposed into different short scales of windows for the higher frequencies, and long window scales for the low frequencies. Electrical signals such as currents and voltages are not free from harmonics; the Discrete Wavelet Transform is very effective. Its formulation can be written as follows:

$$\Psi_{S,\tau}(t) = S^{-1/2} \cdot \Psi(t - \tau/S); S > 0; S \in R \quad (16)$$

where the mother wavelet Ψ is expanded or contracted by the scale factor S ($S^{-1/2} \cdot \Psi(t/S)$). Such a mother wavelet is inversely proportional to the frequency and is shifted by the shift factor τ(Ψ(t − τ)) [19]. The mother wavelet chosen to develop the DWT analysis must have good features to remove harmonics as well as high performance when extracting the main characteristics of the studied signal. There are several mother wavelets such as Harr, Daubechies, Biorthogonal, Coiflets, etc. The number of decomposition steps is chosen function of the sampling frequency of the original signal. The first decomposition has two elements: a high-frequency element D_1 and a low-frequency element A_1. As a function of the sampling frequency f_s, the frequency band of D_1 element is $f_s/2$–$f_s/4$ Hz, whereas the frequency band of A_1 element is $f_s/4$–0 Hz. In the second decomposition, the A_1 element is decomposed into D_2 element for the high-frequency band ($f_s/4$–$f_s/8$ Hz) and A_2 element for the low-frequency band ($f_s/8$–0 Hz). This process is repeated until the desired frequency band reached allows the right information of the evaluated signal to be extracted. In Figure 7, the decomposition developed by the wavelet transform can be seen.

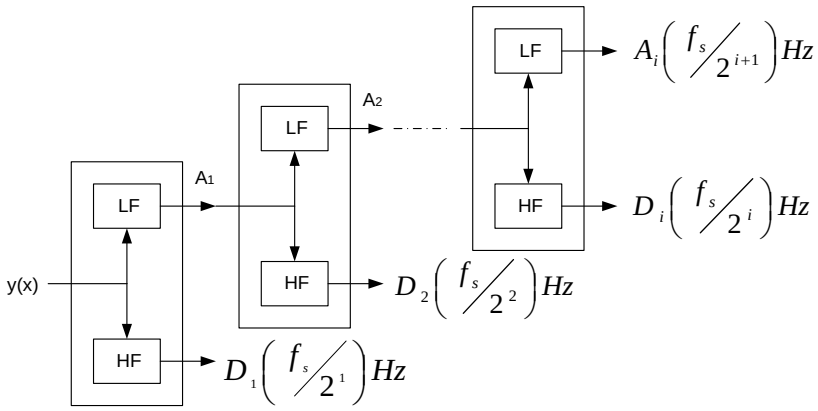

Figure 7. Wavelet transform. Frequency bands related to decomposition steps.

The Daubechies 2 mother wavelet, dB2, has been selected, as it has good characteristics to classify the magnitude of the D_1 component [20] when the ground fault is located at the overhead or cable side of the line. The threshold for D_1 value components has been selected to 50 to block the auto-reclosing order when its value is higher. The variable W represents its value in the algorithm (Figure 8).

4.3. Algorithm of New Auto-Reclosing Blocking Method

Figure 8 shows the algorithm used to determine the location of the ground fault is. The analysis of ΔL1S1, ΔL2S2 and ΔL3S3 is developed in parallel with a wavelet analysis that evaluates the maximum values of the dB2-cD1 coefficients for such ΔL1S1, ΔL2S2 and ΔL3S3. The values of the dB2-cD1 coefficients are analyzed, and the variable W is obtained.

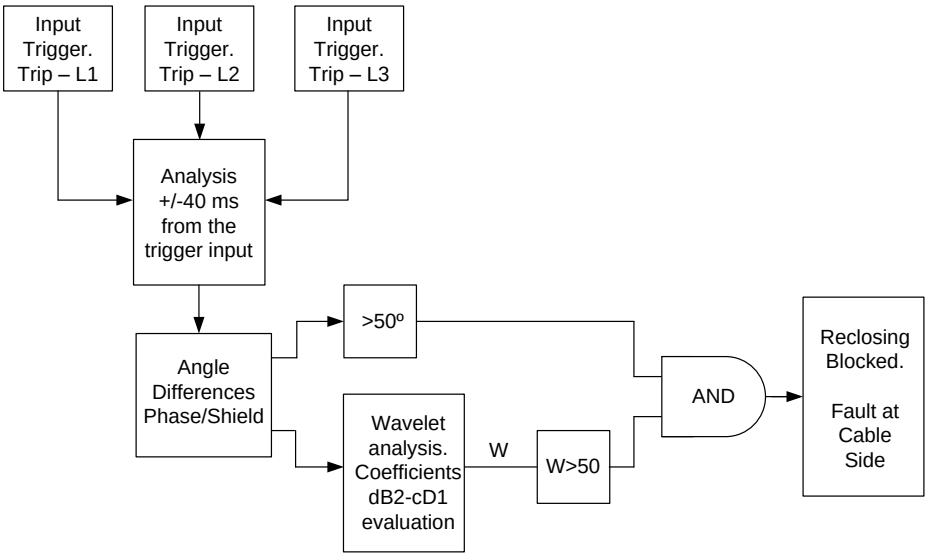

Figure 8. Algorithm of the new auto-reclosing blocking method.

5. Analysis of Simulation Results

The proposed auto reclosing blocking method was simulated using Simulink® in a typical power distribution network presented as a case study. An equivalent "*pi*" model for lines was used as well as power transformers rated 66/20 kV, 20 MVA with Dyn1 connection group and distribution transformers rated 20/0.4 kV, 630 kVA and connection group Dyn11. Loads in these distribution transformers were considered up to 600 kVA with standard power factors from 0.85 inductive to 1. The grid scheme used has one overhead distribution line with a total length of 24 km. The "*pi*" parameters of the overhead line without ground wire have the following values: $R_0 = 0.831\ \Omega/km$, $R_1 = 0.687\ \Omega/km$, $L_0 = 0.00486\ H/km$, $L_1 = L_2 = 0.001383\ H/km$, $C_0 = 4.24 \times 10^{-9}\ F/km$, $C_1 = C_2 = 8.89 \times 10^{-9}\ F/km$. The conductor type is LA-56 with diameter $\Phi_{LA56} = 9.45$ mm, $R_{LA56} = 0.616\ \Omega/km$, $I_{max} = 199.35$ A and geometric mean distance GMD = 2.53 m. The underground cable used is RHZ1 2OL 12/20 kV whose main features are: $\Phi_{Cable\text{-}core} = 13.82$ mm, $S_c = 150\ mm^2$, $S_s = 16\ mm^2$, $R = 0.188\ \Omega/km$, $\Phi_{ext} = 34.4$ mm. A cable length from 600–1200 m was chosen. The shields of these cables are connected in SB, whereas the overhead line considers span lengths of 100 m. The ground resistance at the transition takes a typical value of 12 Ω and at the cable end substation 0.5 Ω. The model used is shown in Figure 9.

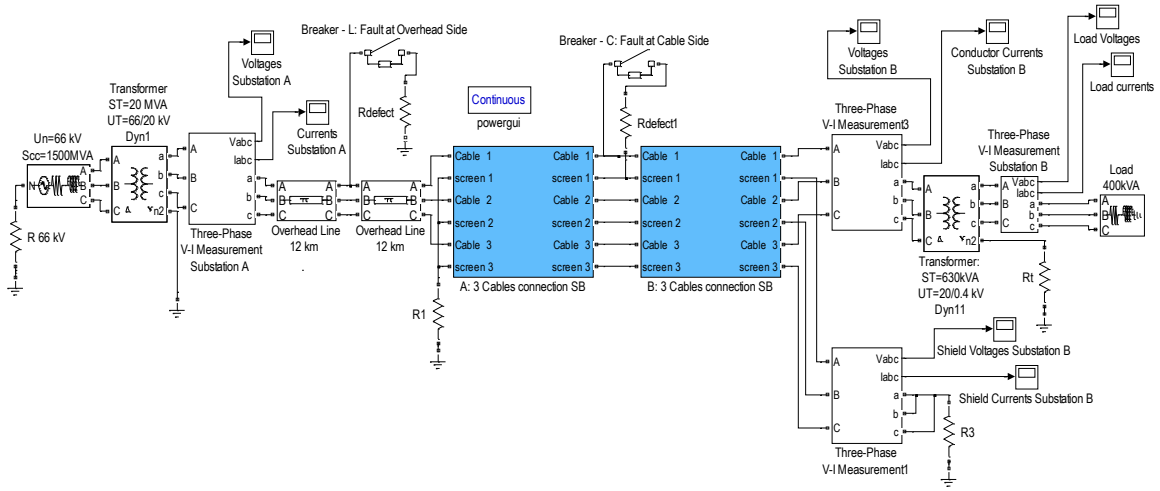

Figure 9. New auto-reclosing blocking method: model implemented.

5.1. Angular Difference Analysis in Power Distribution Networks Solidly Grounded at the Overhead Side and Isolated at the Cable End Side

The angular differences ΔL1S1, ΔL2S2 and ΔL3S3 between currents in the shields and in the active part of the cables in a system ungrounded at the cable side (typical power transformer in delta connection) and solidly grounded at the overhead side have been all simulated during normal operation of the power distribution network without ground fault and with it along different position at the overhead side and at the cable side. Multiple simulations show that the classification of the ground faults turns out to be:

- Ground fault in the overhead side: if ΔL1S1, ΔL2S2 and ΔL3S3 are less than 50°, normally in all phases.
- Ground fault in the cable line side: if at least one of ΔL1S1, ΔL2S2 or ΔL3S3 is clearly over 50°.

Figures 10 and 11 show how the variations of ΔL1S1, ΔL2S2 and ΔL3S3 are when the power distribution network suffers a ground fault in phase L1 at the overhead line side 12 km from the transition, and at the cable line side in its central position in t = 200 ms. The overhead line has a total length of 24 km and the cable 600 m.

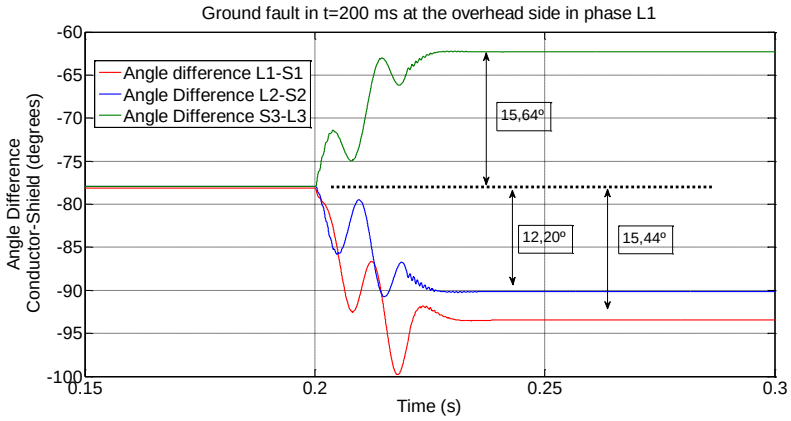

Figure 10. Angular differences with ground fault at the overhead side in phase L1.

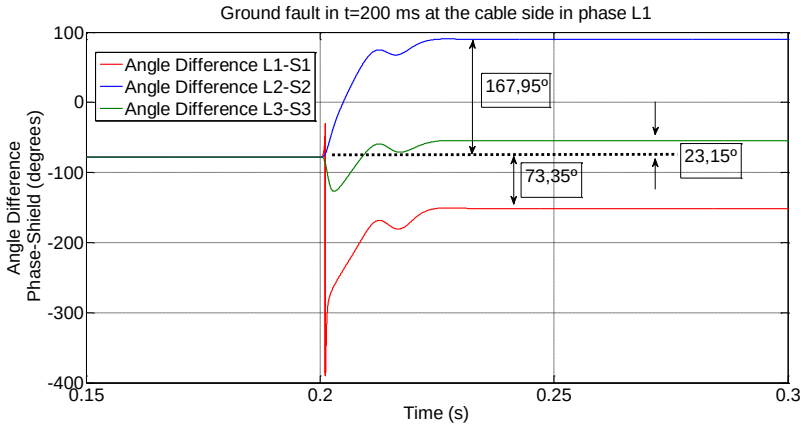

Figure 11. Angular differences with ground fault at the cable line side in phase L1.

Considering distances from the transition, Table 1 shows the results of the variation in ΔL1S1, ΔL2S2 and ΔL3S3 from only 1 m to more than 10 km in the overhead line side, and from 1 to 599 m in the cable line side. It can be seen how the variations of ΔL1S1, ΔL2S2 and ΔL3S3 are reduced when the ground fault occurs at the overhead line side and are very high when the ground fault happens t the cable line side.

Table 1. Phase angle variation with ground faults at the overhead and cable line sides.

Fault at Overhead Line Side				Fault at Cable Line Side			
Distance from Transition	Fault in Phase L1			Distance from Transition	Fault in Phase L1		
	Variation in Phase Angles				Variation in Phase Angles		
	ΔL1S1	ΔL2S2	ΔL3S3		ΔL1S1	ΔL2S2	ΔL3S3
1 m	15.18°	10.98°	15.26°	1 m	73.69°	168.62°	24.03°
10 m	15.16°	10.99°	15.24°	10 m	73.72°	168.65°	24.05°
100 m	15.17°	11.01°	15.26°	50 m	73.75°	168.61°	24.12°
1000 m	15.18°	11.05°	14.27°	100 m	73.71°	168.52°	23.73°
5000 m	15.25°	11.33°	15.37°	300 m	73.35°	167.95°	23.15°
>10,000 m	15.44°	12.20°	15.64°	599 m	67.32°	157.11°	27.67°
Fault at Overhead Line Side				**Fault at Cable Line Side**			
Distance from Transition	Fault in Phase L2			Distance from Transition	Fault in Phase L2		
	Variation in Phase Angles				Variation in Phase Angles		
	ΔL1S1	ΔL2S2	ΔL3S3		ΔL1S1	ΔL2S2	ΔL3S3
1 m	15.34°	15.33°	10.81°	1 m	24.02°	73.72°	168.58°
10 m	15.35°	15.34°	10.88°	10 m	24.10°	73.70°	168.59°
100 m	15.34°	15.33°	10.87°	50 m	23.92°	73.71°	168.47°
1000 m	15.37°	15.36°	10.85°	100 m	23.85°	73.79°	168.42°
5000 m	15.48°	15.45°	11.20°	300 m	22.99°	73.55°	167.65°
>10,000 m	15.67°	15.56°	11.72°	599 m	27.87°	67.51°	157.52°
Fault at Overhead Line Side				**Fault at Cable Line Side**			
Distance from Transition	Fault in Phase L3			Distance from transition	Fault in Phase L3		
	Variation in Phase Angles				Variation in Phase Angles		
	ΔL1S1	ΔL2S2	ΔL3S3		ΔL1S1	ΔL2S2	ΔL3S3
1 m	11.78°	15.41°	15.25°	1 m	168.61°	24.01°	73.31°
10 m	11.79°	15.42°	15.22°	10 m	168.62°	24.02°	73.70°
100 m	11.77°	15.43°	15.23°	50 m	168.51°	23.92	73.72°
1000 m	11.82°	15.45°	15.25°	100 m	168.40°	23.75°	73.31°
5000 m	12.13°	15.55°	15.33°	300 m	168.12°	23.11°	73.55°
>10,000 m	12.66°	15.73°	15.45°	599 m	157.36°	67.78°	68.01°

5.2. Wavelet Analysis in a Power Distribution Network Solidly Grounded at the Overhead Line Side and Isolated at the Cable End Side

The simulation results of this configuration included in Table 2 show that the angular difference when the ground fault has happened in the overhead side has dB2-cD1 coefficients lower than 0.1, and over 100 when the fault is in the e line side. Figures 12 and 13 show the results obtained for ground faults in phase L1 at the overhead line side and cable lines side respectively.

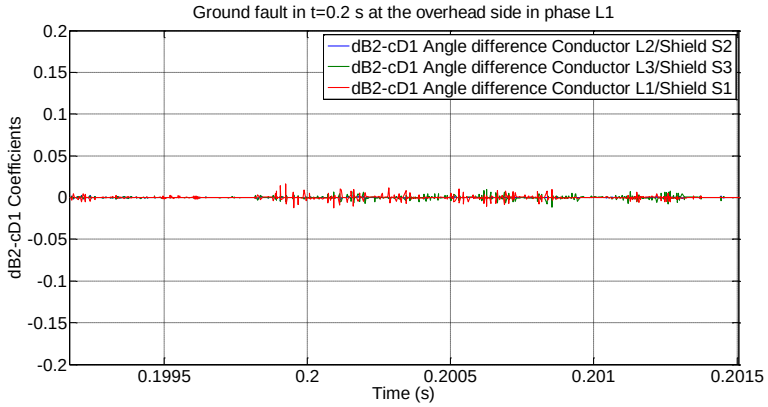

Figure 12. Wavelet dB2-1-cD1 coefficients of the angular difference signals with ground fault in phase L1 at the overhead side 12 km from the transition.

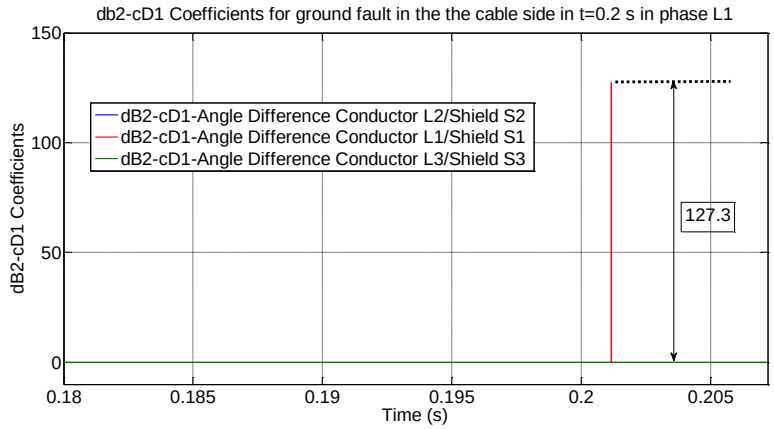

Figure 13. Wavelet dB2-1-cD1 coefficients of the angular difference signals with ground fault in phase L1 at the cable line side 300 m from the transition.

Table 2. Wavelet analysis: simulation results. Ground faults at the overhead and cable line sides. Overhead line side solidly grounded and cable line side isolated. Phase currents measured in the conductors (L1, L2, L3) and in their shields (S1, S2, S3).

Fault at Overhead Line Side				**Fault at Cable Line Side**			
Distance from Transition	**Fault in Phase L1**			**Distance from Transition**	**Fault in Phase L1**		
	W (dB2-cD1 Coefficients)				**W (dB2-cD1 Coefficients)**		
	ΔL1S1	**ΔL2S2**	**ΔL3S3**		**ΔL1S1**	**ΔL2S2**	**ΔL3S3**
1 m	0.0068	0.0067	0.0065	1 m	173.88	0.0134	0.0096
10 m	0.0039	0.0041	0.0041	10 m	173.89	0.0123	0.0097
100 m	0.0033	0.0038	0.0039	50 m	127.32	0.0113	0.0094
1000 m	0.0027	0.0029	0.0025	100 m	127.32	0.0119	0.0097
5000 m	0.0019	0.0024	0.0019	300 m	127.31	0.0128	0.0089
>10,000 m	0.0014	0.0016	0.0013	599 m	123.67	0.02784	0.0332
Fault at Overhead Line Side				**Fault at Cable Line Side**			
Distance from Transition	**Fault in Phase L2**			**Distance from Transition**	**Fault in Phase L2**		
	W (dB2-cD1 Coefficients)				**W (dB2-cD1 Coefficients)**		
	ΔL1S1	**ΔL2S2**	**ΔL3S3**		**ΔL1S1**	**ΔL2S2**	**ΔL3S3**
1 m	0.0067	0.0064	0.0069	1 m	0.0095	173.90	0.0136
10 m	0.0044	0.0039	0.0042	10 m	0.0098	173.90	0.0122
100 m	0.0037	0.0031	0.0039	50 m	0.0095	127.30	0.0114
1000 m	0.0029	0.0022	0.0028	100 m	0.0098	127.30	0.0120
5000 m	0.0021	0.0017	0.0022	300 m	0.0088	127.31	0.0130
>10,000 m	0.0016	0.0011	0.0015	599 m	0.0333	123.70	0.02782
Fault at Overhead Line Side				**Fault at Cable Line Side**			
Distance from Transition	**Fault in Phase L3**			**Distance from Transition**	**Fault in Phase L3**		
	W (dB2-cD1 Coefficients)				**W (dB2-cD1 Coefficients)**		
	ΔL1S1	**ΔL2S2**	**ΔL3S3**		**ΔL1S1**	**ΔL2S2**	**ΔL3S3**
1 m	0.0066	0.0064	0.0065	1 m	0.0135	0.0094	173.91
10 m	0.0044	0.0045	0.0037	10 m	0.0121	0.0097	173.91
100 m	0.0037	0.0039	0.0030	50 m	0.0113	0.0097	127.29
1000 m	0.0029	0.0031	0.0024	100 m	0.0121	0.0099	127.29
5000 m	0.0023	0.0023	0.0018	300 m	0.0131	0.0087	127.30
>10,000 m	0.0016	0.0015	0.0013	599 m	0.02783	0.0334	127.71

6. Experimental Results

Different laboratory tests were developed in order to test the validity of the new auto-reclosing blocking method, and to check the computer simulation results obtained.

6.1. Experimental Setup

The tests were carried out on a solidly earthed source supplied by a power transformer rated 800 VA, 400/100 Vac and Dyn1 connection group. Two line module emulators with equivalent circuit "*pi*" were used with the following features: R = 88.48 mΩ, L = 4 mH and C = 4 μF each capacitor. The real cable used has the following characteristics: R = 1.8 Ω, L = 22 mH and C = 4.9 nF with a total cable length of 300 m. Two overcurrent protection relays of type MRI4 by Woodward-Seg are used as disturbance recorders to store the values of the currents flowing in the active conductors and the shields of the cables. A second transformer rated 800 VA, 400/100 Vac and Dyn11 is used to supply different loads in delta connection. Figure 14 shows the experimental setup and the RLC features of the line module emulators used.

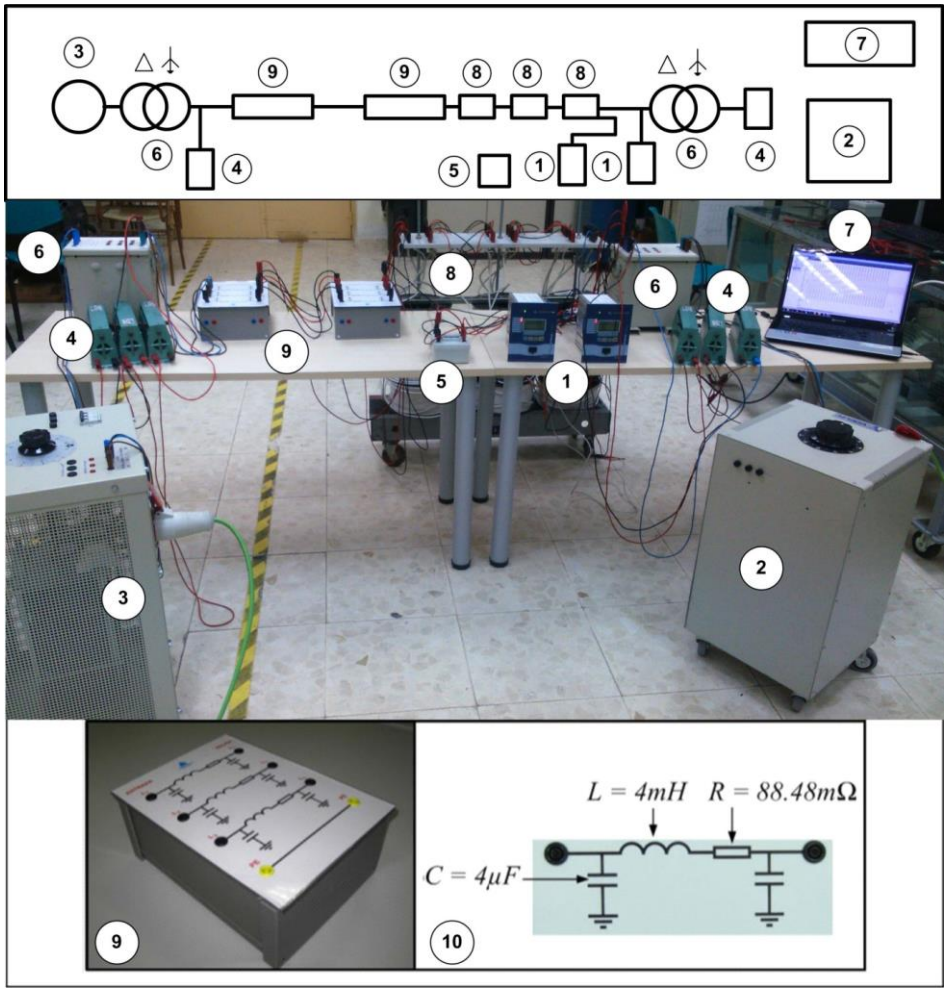

Figure 14. Experimental setup. 1: Protection relays; 2: Auxiliary power supply; 3: Power supply; 4: Loads; 5: Ground fault switch; 6: Transformer; 7: PC; 8: Cables; 9: Line modules; 10: RLC parameters of the line modules (9) used.

Several single ground faults at all phases in lines and cables were carried out in the network erected in the laboratory. Tests were developed at 100 V phase-to-phase voltage and load currents of less than 1 A with different cosϕ values. The positions where the ground faults were developed (indicated in Figure 15) are represented schematically in Figure 16.

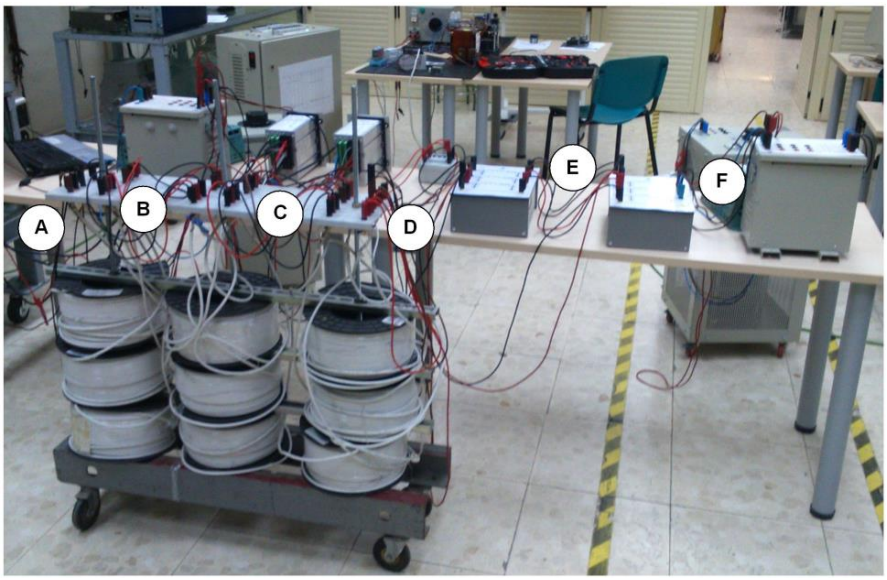

Figure 15. Ground fault positions. A: At the end of the cable; B: Between the first and second sections of the cables; C: Between the second and third sections of the cables; D: In the transition at the end of the cables; E: Between the first and second trams of the line modules; F: Behind the two line modules.

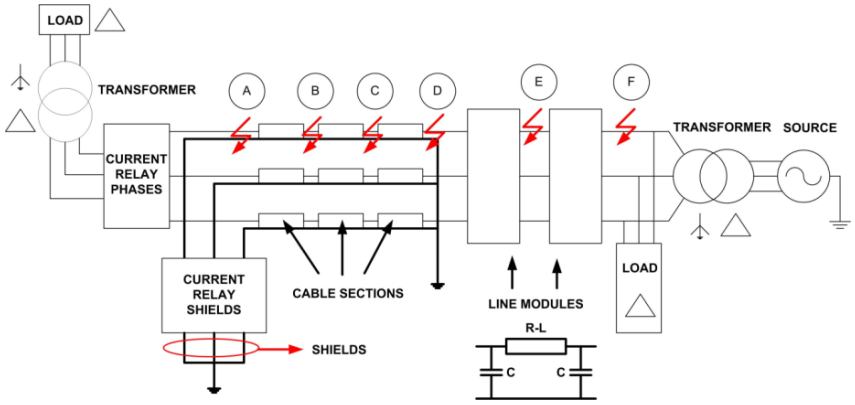

Figure 16. Ground fault positions: schematic representation.

6.2. Angle Analysis of the Experimental Power Distribution

In the experimental circuit test shown in Figure 16, the network is solidly grounded at the beginning of the overhead line side whereas the transformer which supplies the load has a delta connection in its higher voltage side. The angular differences ΔL1S1, ΔL2S2 and ΔL3S3 obtained in the tests in a system ungrounded at the cable line side and solidly grounded at the overhead line side were:

- Ground fault in overhead side: if the angular difference between the active and respective shield of the currents in the phase with a fault is less than 50°.
- Ground fault in the cable line side: if the angular difference between the active and respective shield of the currents in the phase with a fault is clearly over 50°.

Figures 17 and 18 show the angular difference between phase and shield currents when there is a ground fault in phase L1 in the overhead side at fault point E, and at the cable line side in fault point C. The test results included in Tables 3–5 show values of variations in ΔL1S1, ΔL2S2 and ΔL3S3 over 50° and below 50° when the ground fault is developed at the overhead line side.

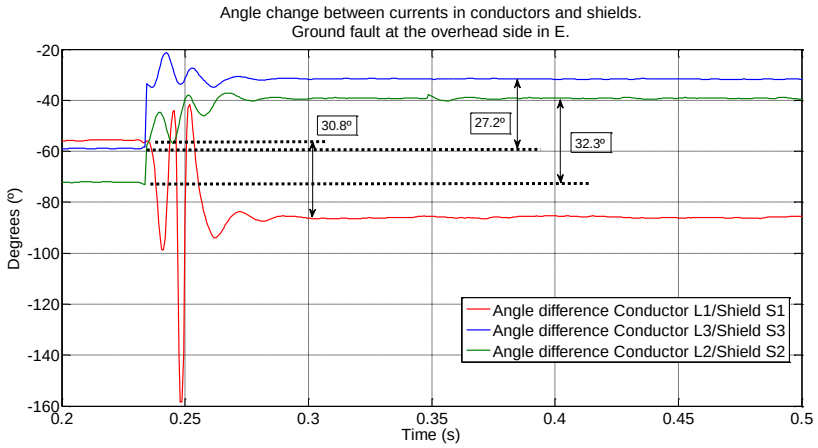

Figure 17. Angular differences with ground fault at the overhead side in phase L1. Fault point E.

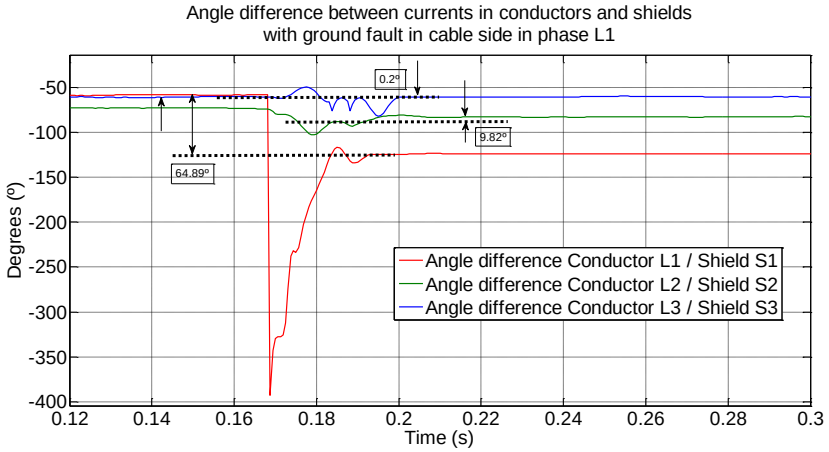

Figure 18. Angular differences with ground fault at the cable line side in phase L1. Fault point C.

Tables 3–5 show the results of ΔL1S1, ΔL2S2 and ΔL3S3 in ground fault locations A, B, C, D in the cable line side, and in locations E and F at the overhead line side.

Table 3. Ground fault at overhead and cable line sides in phase L1. Variation in phase angles between currents in the conductors and their respective shields.

Fault at Cable Line Side			
Place of the Fault	**Fault in Phase L1**		
	Variation in Phase Angles		
	ΔL1S1	**ΔL2S2**	**ΔL3S3**
A	66.32°	11.02°	0.33°
B	65.93°	10.24°	0.26°
C	64.89°	9.82°	0.20°
D	64.25°	9.31°	0.18°
Fault at Overhead Line Side			
Place of the Fault	**Fault in Phase L1**		
	Variation in Phase Angles		
	ΔL1S1	**ΔL2S2**	**ΔL3S3**
E	30.80°	32.31°	27.16°
F	29.12°	31.86°	26.02°

Table 4. Ground fault at overhead and cable line sides in phase L2. Variation in phase angles between currents in the conductors and their respective shields.

Fault at Cable Line Side			
Place of the Fault	**Fault in Phase L2**		
	Variation in Phase Angles		
	ΔL1S1	**ΔL2S2**	**ΔL3S3**
A	0.29°	66.45°	12.08°
B	0.25°	65.99°	10.93°
C	0.21°	65.02°	9.88°
D	0.16°	64.67°	9.33°
Fault at Overhead Line Side			
Place of the Fault	**Fault in Phase L2**		
	Variation in Phase Angles		
	ΔL1S1	**ΔL2S2**	**ΔL3S3**
E	1.29°	31.78°	16.29°
F	1.11°	25.11°	12.11°

Table 5. Ground fault at overhead and cable line sides in phase L3. Variation in phase angles between currents in the conductors and their respective shields.

Fault at Cable Line Side			
Place of the Fault	**Fault in Phase L3**		
	Variation in Phase Angles		
	ΔL1S1	**ΔL2S2**	**ΔL3S3**
A	12.58°	0.30°	67.34°
B	10.13°	0.26°	66.86°
C	9.01°	0.20°	65.78°
D	8.92°	0.18°	64.02°
Fault at Overhead Line Side			
Place of the Fault	**Fault in Phase L3**		
	Variation in Phase Angles		
	ΔL1S1	**ΔL2S2**	**ΔL3S3**
E	17.34°	1.35°	32.45°
F	14.22°	1.18°	23.67°

6.3. Wavelet Analysis of the Experimental Power Distribution Network

The cD1 coefficients obtained from the angular differences in the tests between currents in the shields and in the active cables in a system that is ungrounded at the cable line side and solidly grounded at the overhead line side were:

- Ground fault in overhead line side: if the cD1 coefficient values are lower than 50 in all phases.
- Ground fault in the cable line side: if the cD1 coefficient values are much higher than 50, i.e., 100 or more.

Figure 19 shows the dB2-cD1 coefficient values of the angular difference between phase and shield currents when there is a ground fault in phase L1 in the overhead line side at fault point E. These values of the dB2-cD1 coefficients are higher than the values obtained from the simulated case shown in Figure 12. This difference is related to the physical disposal of the real cables in the laboratory which are wound in coils instead of been laid under the ground as they were considered in the simulated model. Figure 20 shows at the cable line side in fault point C. Table 6 shows the big differences in the values of the dB2-cD1 coefficients from ground faults at the overhead line side to ground faults at the cable side.

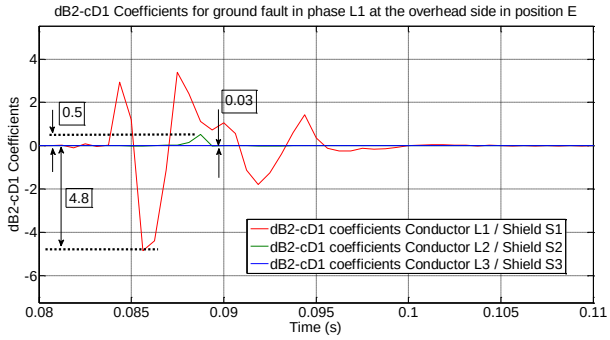

Figure 19. Wavelet analysis of the angular differences with a ground fault at the overhead line side in phase L1. Fault point E.

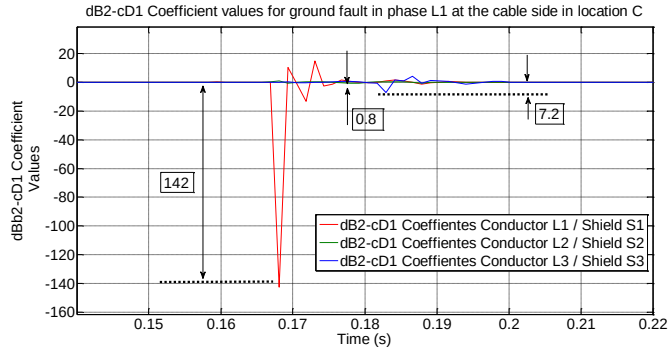

Figure 20. Wavelet analysis of the angular differences with a ground fault at the cable line side in phase L1. Fault point C.

Table 6. Ground fault at overhead and cable line sides. Wavelet analysis: experimental results. Overhead line side solidly grounded and cable line side isolated.

Fault at Cable Line Side				**Fault at Overhead Line Side**			
Location of the Fault	**Fault in Phase L1**			**Location of the Fault**	**Fault in Phase L1**		
	W (dB2-cD1 Coefficients)				**W (dB2-cD1 Coefficients)**		
	ΔL1S1	**ΔL2S2**	**ΔL3S3**		**ΔL1S1**	**ΔL2S2**	**ΔL3S3**
A	152.24	2.45	18.29	E	4.80	0.03	0.50
B	145.88	1.96	14.12				
C	142.01	0.80	7.21	F	4.66	0.02	0.42
D	136.54	0.69	4.75				
Fault at Cable Line Side				**Fault at Overhead Line Side**			
Location of the Fault	**Fault in Phase L2**			**Location of the Fault**	**Fault in Phase L2**		
	W (dB2-cD1 Coefficients)				**W (dB2-cD1 Coefficients)**		
	ΔL1S1	**ΔL2S2**	**ΔL3S3**		**ΔL1S1**	**ΔL2S2**	**ΔL3S3**
A	20.04	154.31	3.01	E	0.04	4.88	0.59
B	16.59	148.22	2.42				
C	9.92	143.67	0.89	F	0.03	4.72	0.48
D	6.82	138.08	0.82				
Fault at Cable Line Side				**Fault at Overhead Line Side**			
Location of the Fault	**Fault in Phase L3**			**Location of the Fault**	**Fault in Phase L3**		
	W (dB2-cD1 Coefficients)				**W (dB2-cD1 Coefficients)**		
	ΔL1S1	**ΔL2S2**	**ΔL3S3**		**ΔL1S1**	**ΔL2S2**	**ΔL3S3**
A	2.66	19.44	153.01	E	0.47	0.04	4.34
B	1.49	15.18	144.78				
C	0.81	6.96	140.12	F	0.51	0.02	4.11
D	0.52	3.97	134.96				

7. Conclusions and Future Work

A new auto-reclosing blocking method for combined overhead-cable lines in power distribution networks has been presented in this article. This method is applicable when the transition overhead-cable is close to the substation where the measurements of currents in shields and conductors are done. The shields of the cables are grounded at both ends. The proposed ground fault auto-reclosing method is based on two analyses. The first evaluates the difference between the currents in the active part of the cable and those in the shields, whereas the second analysis uses the wavelet Daubechies dB2 and extracts the coefficients cD1 from the same differences used in the first analysis. If the argument differences between the currents in the conductors of the cable and those in the shields have a phase variation just after a ground fault occurs with higher values than a reference difference and, at the same time, the Daubechies-cD1 coefficients of such differences have values over a reference threshold, then a ground fault has occurred in the cable line side and the reclosing is blocked. On the other hand, if the phase variation just after a ground fault takes place between the currents in the conductor of the cable and those in the shields has lower values than a reference argument difference, and the Daubechies-cD1 coefficients of such a variation have very small values, the ground fault has occurred at the overhead line side, and the reclosing is released.

The simulations turned out to be totally satisfactory and the experimental results of the laboratory tests showed that the localization of the ground fault is correct. This novel technique has important advantages compared to up-and-running ground fault detection systems:

- It discriminates whether a ground fault happens at the overhead line side or cable line side;
- It does not use any voltage measurement;
- It does not use any directional criterion;
- It does not use the residual ground fault current to localize the ground fault;
- It does not consider any distance calculation to localize the ground fault;
- It does not consider any differential tripping criterion to localize the ground fault.

The aforementioned advantages of the proposed technique make it easier to determine where the ground fault is and, consequently, to allow the protection relay to make the best possible use of the auto-reclosing functionality. The stability of the grid is also improved because wrong reclosing commands are not sent while ground fault conditions are active.

Acknowledgments: The authors wish to thank the reviewers for their helpful and constructive comments.

Author Contributions: Ricardo Granizo Arrabé developed the study and included all the mathematical formulations of the cables in the simulated models. Carlos Antonio Platero Gaona and Fernando Álvarez Gómez performed the laboratory tests and checked the validity of the new auto-reclosing blocking method. Emilio Rebollo López revised and improved the Matlab-Simulink® model. All the authors contributed to writing this article, including their conceptual approaches to the solution obtained.

Conflicts of Interest: The authors declare no conflicts of interest.

Abbreviations

The following abbreviations are used throughout the article:

AC	Alternating Current
AND	Logical Function
CT	Current Transformer
cD	Detail Coefficient
DWT	Discrete Wavelet Transformation
Dyn1	Delta-Star with Ground Connection of Power Transformer
Dyn11	Delta-Star with Ground Connection of Distribution Transformer
dB2	Daubechies 2 Mother Wavelet
GMD	Geometric Mean Distance
HF	High Frequency
LF	Low Frequency
SB	Single Bonding
ΔLiSj	variation of the argument difference between the current in phase i and that in shield j

Indices and Sets

i	Index of each conductor
j	Index of each shield
k	Index of each level of detail coefficients in wavelet analysis
m	Index of each level of approximation coefficients in wavelet analysis

Parameters

A, B, C, D, E, F	ground fault situation in laboratory tests
A_m	approximation level "m" for wavelet analysis
C_0	zero sequence capacitance value
C_1	direct sequence capacitance value
C_2	negative sequence capacitance value
D_e	equivalent distance for ground return
Dm	detail level "m" of wavelet analysis
f	frequency
f_s	sampling frequency
I_0	ground fault current
I_1	current in conductor 1
I_2	current in conductor 2
I_3	current in conductor 3
j	imaginary part of complex vector
L	length of the conductor
L1	phase one
L2	phase two
L3	phase three
L_0	zero sequence inductance value
L_1	direct sequence inductance value
L_2	negative sequence inductance value
ln	logarithm
R	real part or resistance of any impedance
$R_{C(ac)}$	resistance of the conductor in AC
R_0	zero sequence resistance value
R_1	direct sequence resistance value
r_{oc}	outer radius of the conductor
r_s	average radius of the shield
$R_{S(ac)}$	resistance of the shield in AC
R_{SA}	ground resistance of substation A
R_{SB}	ground resistance of substation B
R_t	ground resistance of any tower of distribution lines
S1	shield of conductor in phase L1
S2	shield of conductor in phase L2
S3	shield of conductor in phase L3
S_{CS}	distance between axes of conductor and shield
S_{SS}	distance between axes of shields
t_A	tripping time for impedance zone A
t_B	tripping time for impedance zone B
t_C	tripping time for impedance zone C
U	voltage difference between shield ends
U_{1C}	induced voltage in shield 1 of conductor 1 due to circulating currents in conductors
U_{2C}	induced voltage in shield 2 of conductor 2 due to circulating currents in conductors
U_{3C}	induced voltage in shield 3 of conductor 3 due to circulating currents in conductors
U_{1S}	induced voltage in shield 1 of conductor 1 due to circulating currents in shields
U_{2S}	induced voltage in shield 2 of conductor 2 due to circulating currents in shields
U_{3S}	induced voltage in shield 3 of conductor 3 due to circulating currents in shields
U_0	residual voltage
X	imaginary part or reactance of any impedance
Z_C	self-impedance of a conductor
Z_{CS}	mutual impedance between conductor and shield
Z_I	impedance zone I
Z_L	line impedance
Z_S	self-impedance of a shield
Z_{SS}	mutual impedance between shields

References

1. Tleis, N. *Power Systems Modelling and Fault Analysis*, 1st ed.; Newnes: Oxford, UK, 2008.
2. Saha, M.M.; Izykowsky, J.; Rosolowsky, E. *Fault Location on Power Networks*; Springer: Berlin, Germany, 2009.
3. Horowitz, S.H.; Phadke, A.G. *Power System Relaying*, 3rd ed.; Wiley: New York, NY, USA, 2008.
4. L'Abbate, A.; Fulli, G.; Starr, F.; Peteves, S. *Distributed Power Generation in Europe: Technical Issues for Further Integration*; JRC European Commission Scientific and Technical Report, EUR 23234 EN; Office for Official Publications of the European Communities: Luxembourg, 2007.
5. Tamo, T.; Voufo, J. Fault diagnosis on medium voltage (MV) electric power distribution networks: The case of the downstream network of the AES-SONEL Ngousso sub-station. *Energies* **2009**, *2*, 243–257.
6. Li, P.; Zhang, B.H.; Hao, Z.G.; Rao, Y.F.; Wang, Y.T.; Bo, Z.Q.; Klimek, A.; Zhao, Q.; He, W. Optimal Reclosing Time of Transmission Lines and its Application in Real Power System. In Proceedings of the 9th International Conference on Developments in Power System Protection, Glasgow, UK, 17–20 March 2008.
7. He, R.W. A New Approach to the Calculation of Reclosing Time for Adaptive Auto-reclosure. In Proceedings of the 2010 Asia-Pacific Power and Energy Engineering Conference, Chengdu, China, 28–31 March 2010.
8. Zoro, R.; Mefiardhi, R. Lightning performance on overhead distribution lines: Field observation at West Java—Indonesia. In Proceedings of the 7th International Power Engineering Conference, Singapore, 29 November–2 December 2005.
9. Yu, Y.Z.; Qin, J.; Li, G.X.; Chen, S.Y.; Li, J.; Chen, Y.Y. A Survey on Fault Location Methods for Hybrid Transmission Lines Consisting of Power Cables and Overhead Lines. *Power Syst. Technol.* **2006**, *30*, 64–69.
10. Standard CEI_60909-3. Short-Circuit Current Calculation in Three-Phase a.c. Systems. Part 3. Currents during Two Separate Simultaneous Single Phase Line-to-Earth Short Circuits and Partial Short-Circuit Currents Flowing through Earth. Available online: https://webstore.iec.ch/publication/3890 (accessed on 17 November 2016).
11. Radojevic, Z.; Terzija, V. Two Terminals Numerical Algorithm for Fault Distance Calculation and Fault Analysis. In Proceedings of the 2006 IEEE PES Power Systems Conference and Exposition, Atlanta, GA, USA, 29 October–1 November 2006.
12. Zhou, Y.; Xu, G.; Chen, Y. Fault Location in Power Electrical Traction Line System. *Energies* **2012**, *5*, 5002–5018. [CrossRef]
13. Terzija, V.V.; Dobrijevic, D.M. Short Circuit Studies in Transmission Networks Using Improved Fault Model. In Proceedings of the IEEE Lausanne Power Tech, Lausanne, Switzerland, 1–5 July 2007.
14. Simón, P.; Garnacho, F.; Moreno, J.; González, A. *Cálculo y Diseño de Líneas Eléctricas de Alta Tensión*; Ibergarceta Publicaciones, S.L.: Madrid, Spain, 2011.
15. Magnago, F.H.; Abur, A. Fault location using wavelets. *IEEE Trans. Power Deliv.* **1998**, *13*, 1475–1480. [CrossRef]
16. Costa, F.B.; Souza, B.A.; Brito, N.S.D. Real-time classification of transmission line faults based on maximal overlap discrete wavelet transform. In Proceedings of the 2012 IEEE/PES Transmission and Distribution Conference and Exposition, Orlando, FL, USA, 7–10 May 2012.
17. Han, J.; Crossley, P.A. Fault location on a mixed overhead and underground transmission feeder using a multiple-zone quadrilateral impedance relay and a double-ended travelling wave fault locator. In Proceedings of the 2014 12th International Conference on Developments in Power System Protection, Copenhagen, Denmark, 31 March–3 April 2014.
18. Huang, J.G.; Hu, X.Y.; Li, X.S.; Hu, H.M.; Lv, Y.P. A Novel Single-Phase Earth Fault Feeder Detection by Traveling Wave and Wavelets. In Proceedings of the 2006 International Conference on Power System Technology, Chongqing, China, 22–26 October 2006.
19. Martínez, F.; Peris, A.; Rodenas, F. *Tratamiento de Señales Digitales Mediante Wavelets y su uso con Matlab*; Editorial Club Universitario: Alicante, Spain, 2004.
20. Hong, Y.Y.; Wei, Y.H.; Chang, Y.R.; Lee, Y.D.; Liu, P.W. Fault Detection and Location by Static Switches in Microgrids Using Wavelet Transform and Adaptive Network-Based Fuzzy Inference System. *Energies* **2014**, *7*, 2658–2675. [CrossRef]